ACS Photonics

Additions and Corrections

Cite This: *ACS Photonics* 2019, 6, 238−239

pubs.acs.org/journal/apchd5

Correction to "Interminiband Optical Transitions in Graphene Lateral Superlattices"

Yuyu Li and Roberto Paiella*

ACS Photonics **2018** 5 (8), 3331−3337. DOI: 10.1021/acsphotonics.8b00584

We have discovered an error in the numerical code used to compute the absorption and gain spectra presented in our original publication. All the qualitative conclusions made in the article regarding the terahertz optical properties of graphene lateral superlattices (SLs) and their potential device applications remain valid; however, the magnitudes of the predicted effects are weaker. In the following, we include the corrected versions of all the affected figures of the original article and of the Supporting Information document. Related comments from the article discussing the magnitude of parameters extracted from these figures are also updated. All the equations and theoretical models presented in the original publication, as well as the miniband structure calculations, are correct.

Sharp terahertz absorption peaks centered at the frequency of the graphene-SL minigap under study [the local minigap between minibands V3 and V2 near the X point of the mini-Brillouin zone (MBZ)] are again observed in the corrected version of Figure 2. The peak single-pass absorbance $1 - e^{-\alpha}$ computed from these absorption-coefficient spectra is 26% at 5 K and 6% at room temperature. These values remain significantly larger than the interband absorbance of undoped plain graphene (2.3%) and the free-carrier absorbance at the same frequency and carrier density (0.6%).

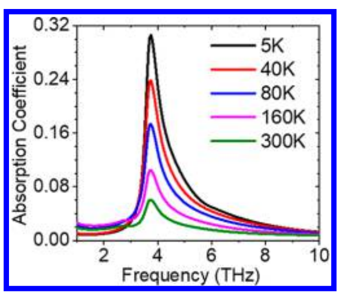

Figure 2. Interminiband absorption in graphene SLs. Absorption spectrum of the SL of Figure 1 under conditions of thermal equilibrium at different temperatures, with the Fermi level at the top of miniband V3.

Broadband electrostatic tunability of the interminiband absorption peak is again obtained in the revised calculations, with a tuning range for the frequency of peak absorption ν_{peak} of about 9 THz in Figure 3a. As the SL potential U_{SL} is increased, the peak absorption coefficient initially increases due to a corresponding increase in the joint density of states between minibands V2 and V3 and then decreases due to a decrease in the optical matrix element between the states involved in the absorption. The maximum modulation depth extracted from the corrected version of Figure 3c is about 27% (from a maximum transmission of nearly unity to a minimum value of about 73%) at a frequency of 4 THz, for a relatively small change in the SL potential of less than 100 meV. In passing, we note that panel b in the revised Figure 3 is the same as in the original publication (since the aforementioned error in the numerical code did not affect the miniband structure calculations), and it is only included here for completeness.

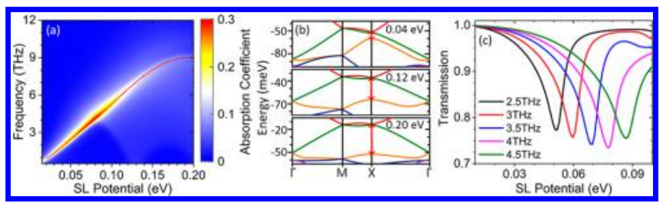

Figure 3. Dynamic tunability of interminiband absorption in graphene SLs. (a) Absorption spectra of the SL of Figure 2 at 5 K for different values of the potential U_{SL}. The dotted line indicates the frequency of peak absorption ν_{peak} as a function of U_{SL}. For each value of U_{SL}, the graphene Fermi level is fixed at the top of miniband V3. (b) Valence miniband structure of the same sample geometry for different values of U_{SL}. (c) Single-pass transmission $e^{-\alpha}$ of the same device at different frequencies plotted as a function of U_{SL}.

The feasibility of terahertz gain under optical pumping is again predicted using the same model and assumptions described in the original article. The optimized pumping parameters used in the revised calculations include a pump intensity of 50 mW focused on a 10 × 10 μm^2 area, and a pump wavelength of 6.7 μm (corresponding to a van Hove singularity in the joint density of states between minibands V3 and C6). The generation rates r_3 and r_2 (i.e., the fraction of incident pump photons absorbed through the creation of holes in minibands V3 and V2, respectively) are computed to be 1.0% and 0.1%, respectively. As indicated in the inset of the corrected Figure 4a, the observed gain again occurs in the absence of a global population inversion between the minibands involved. The maximum gain coefficient g (normalized to the inverse thickness of a graphene single layer) is 0.08 for the graphene-SL configuration of Figure 4a at the longest time constant considered. The corresponding non-normalized value (in units of inverse length) remains extremely large, approximately 2.6×10^6 cm^{-1}. However, because of the ultrasmall graphene thickness (~3 Å), the resulting amplification factor per round trip in a vertical cavity containing the graphene-SL e^{2g} is limited to about 1.2×. Therefore, a more suitable device geometry for the realization of a terahertz laser based on graphene−SL gain media will likely involve a highly confined cavity for in-plane light propagation. As indicated in

Received: December 13, 2018
Published: January 2, 2019

the corrected version of Figure 4b, the frequency of peak gain is again tunable with the SL potential.

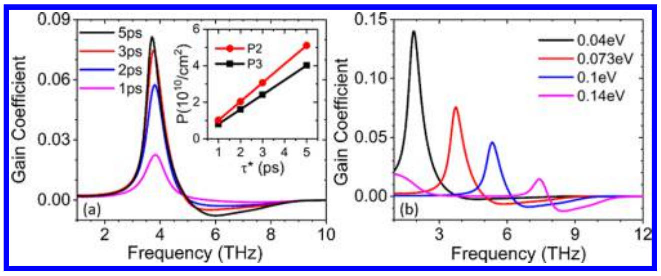

Figure 4. Interminiband gain in optically pumped graphene SLs. (a) Low-temperature gain spectrum of the SL of Figure 1 for different values of the interminiband relaxation lifetime τ^*. Inset: hole densities of minibands V2 and V3 versus τ^*. (b) Gain spectra of the same sample geometry for $\tau^* = 3$ ps and different values of the SL potential U_{SL}.

Pronounced THz absorption peaks are again obtained in the revised calculations even for subpicosecond values of the scattering lifetime τ_{sc}. At the smallest value considered in Figure S1 (200 fs), the corrected peak absorption coefficient is about 0.13, corresponding to a single-pass absorbance through the SL graphene layer of 12%.

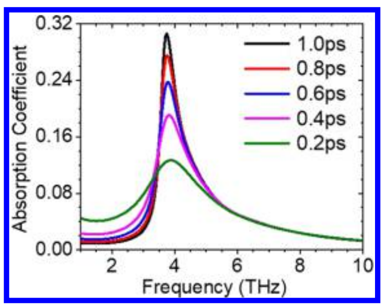

Figure S1. Interminiband absorption spectrum of the same SL of Figure 2 of the main text (at a temperature of 5 K), for different values of the scattering lifetime τ_{sc}.

Figure S2 of the Supporting Information shows simulation results for the interminiband absorption properties of SLs of different period. The key conclusion of these simulations (i.e., that shorter periods are required to access higher peak absorption frequencies) is preserved in the corrected version of the figure. However, we no longer find that at lower frequencies proportionally longer periods can produce somewhat larger peak absorption values.

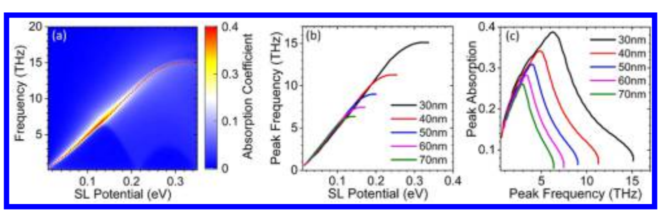

Figure S2. (a) Interminiband absorption spectrum of a SL based on the geometry of Figure 1a of the main text with period $\Lambda = 30$ nm, for different values of the SL potential U_{SL}. (b) Frequency of peak absorption ν_{peak} plotted as a function of U_{SL} for different values of Λ. In all these simulations, the SL is taken to be in thermal equilibrium at 5 K, with the Fermi level aligned to the top of miniband V3. (c) Peak absorption coefficient α_{peak} versus ν_{peak} for different values of Λ.

Figure S3 of the Supporting Information shows the simulation results used to optimize the choice of pump wavelength λ_p for the gain calculations of Figure 4. As discussed in the original publication, λ_p is selected so as to maximize the generation rate r_3 while at the same time keeping r_2 as small as possible. On the basis of the corrected results of these simulations for the SL configuration of Figure 4a, we select a pump wavelength λ_p of 6.7 μm, corresponding to the optical frequency $\nu_p = c/\lambda_p$ shown by the vertical line in Figure S3a,b. The peak in α_{V3} (and therefore in r_3) at this frequency originates from electronic transitions between minibands V3 and C6, mostly involving states along the Γ−X symmetry lines of the MBZ, where the two minibands feature very similar slopes.

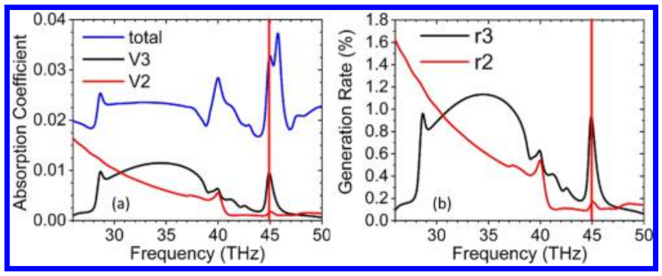

Figure S3. (a) Absorption spectra α_{tot}, α_{V3}, and α_{V2} of an undoped SL based on the geometry of Figure 1a of the main text with $\Lambda = 50$ nm and $U_{SL} = 73$ meV at 5 K. (b) Generation rates r_3 and r_2 computed from the absorption spectra of (a) using eq S1. The vertical lines in (a) and (b) indicate the pump frequency $\nu_p = c/\lambda_p$ selected for the gain calculations on the basis of these simulation results.

Figure S4 of the Supporting Information shows the interminiband gain spectrum of the graphene SL of Figure 4a at different temperatures. Positive gain is again observed in the revised version of this figure even at room temperature, albeit with a rather small peak value of about 0.01 (normalized to the inverse thickness of a graphene single layer). In any case, as already discussed in the original publication, a more definitive determination of the temperature dependence of these gain spectra requires a more detailed knowledge of the intra- and interminiband relaxation dynamics of graphene SLs than presently available.

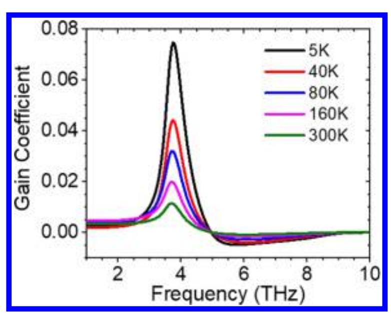

Figure S4. Interminiband gain spectrum of the same SL of Figure 4 of the main text (for an interminiband relaxation lifetime τ^* of 3 ps), at different temperatures.

DOI: 10.1021/acsphotonics.8b01718
ACS Photonics 2019, 6, 238−239